Metastable states of the naive mean-field model for spin glasses at finite temperatures

1990 J. Phys. A: Math. Gen. 23 5915

(http://iopscience.iop.org/0305-4470/23/24/029)

J. Phys. A: Math. Gen. 23 (1990) 5915–5923. Printed in the UK

Metastable states of the naive mean-field model for spin glasses at finite temperatures

K Nishimura, K Nemoto and H Takayama
Institute of Physics, University of Tsukuba, Tsukuba 305, Japan

Received 4 May 1990, in final form 21 August 1990

Abstract. We investigate statistical-mechanical organization of metastable states at finite temperatures in the naive mean-field model for spin glasses by direct numerical analysis on the equations of states of the model. The number of their solutions (metastable states) is shown to agree with the replica prediction developed by Bray and Moore. Furthermore, such sophisticated spin-glass properties as the universal probability law of the non-self-averaging overlap probability of metastable states, which are initially derived for the Sherrington–Kirkpatrick model by means of the replica argument, are demonstrated to be common also to the naive mean-field model.

1. Introduction

The mean-field theory of spin glasses based on the Sherrington–Kirkpatrick (SK) model has revealed various novel properties of its ordered (spin-glass) phase [1]. Among them are the marginal stability of the spin-glass phase, the rugged free-energy structure with many metastable states, the universal probability law of the overlap function of states, and the ultrametric organization of states. Most of these properties have initially been derived by the symmetry-breaking argument in the replica spin space. Later some of them, such as the marginal stability and the existence of many metastable states, have been checked by the analyses in the original spin phase space [2, 3]. For such sophisticated properties as the probability law of the overlap function and the ultrametricity, however, direct confirmation has yet been limited to the metastable states at zero temperature [4, 5]. This is due to the difficulty in numerical analyses of the equations of states of the SK model, i.e., the Thouless–Anderson–Palmer (TAP) equations at finite temperatures [2, 6].

Bray, Sompolinsky and Yu [7] examined another mean-field model for spin glasses, named as the naive mean-field (NMF) model. It is a simplified version of the SK model in the sense that its equations of state consist of only the Weiss field term (the Onsager reaction field term is absent, in contrast to the TAP equations), though the corresponding spin model is rather artificial and complicated. They investigated the spin model mainly by the replica method, and found that the model also shares some spin-glass properties mentioned above. In a recent work [8], two of the present authors investigated the same model by the complementary approach, i.e., by analysing its equations of state (and the corresponding free-energy expression). There the marginal stability of its spin-glass phase is confirmed numerically, and the number of metastable states are evaluated analytically by extending the replica trick first investigated for the

0305-4470/90/245915+09$03.50

TAP equations by Bray and Moore [3]. The results exhibit quite similar dependences on the system size as well as on temperature as those of the SK model. From these results it is natural to expect that the other sophisticated spin-glass properties mentioned above are also common to the NMF model.

The mean-field picture for spin glasses has recently been extended in two directions. One is to investigate whether the picture also holds for realistic spin glasses with short-ranged interactions, in particular, three-dimensional Ising spin-glasses. For the latter systems, the ergodicity breaking at low temperatures was first claimed by Sourlas [9], and the non-self-averaging nature of the overlap probability near below the transition temperature has recently been reported by Caracciolo *et al* [10]. The other direction is to apply the mean-field picture for spin glasses to problems in various fields, such as optimization and neural network models [1]. For an example, in a recent work on the analogue neural network model [11], equations identical to those for NMF model of present interest were examined to determine fixed-point attractors in the model. These extensions are certainly of importance and of interest, but we believe that deeper understanding of the basic mean-field picture is also worth exploring.

The purpose of the present paper is to analyse numerically the nature of the metastable states of the NMF model, taking the advantage of the fact that its equations of state (NMF equations) are much more tractable than the TAP equations. By inspecting all solutions of the NMF equations of finite size, the following properties are confirmed within the accuracy of our numerical analysis: the number of the solutions (metastable states) agrees with our previous result [8] evaluated analytically by the replica trick, the overlap probability $P_J(q)$ (see equation (8) below) and the accumulated probabilities $x_J(q)$ ($\equiv \int_0^q P_J(q\prime)dq\prime$) and $Y_J(q)$ ($\equiv 1 - x_J(q)$) at finite temperatures are not self-averaging, and the probability law of $Y_J(q)$ of the present model almost coincides with the universal probability law predicted for the SK model by the replica method [12]. Although some numerical analyses on $P_J(q)$ at finite temperatures have appeared [10, 13, 14], the present result on $Y_J(q)$ is, to our knowledge, the first numerical evidence for its universal probability law.

In the next section the model and our numerical method are presented. The replica method to analyse the number of metastable states is briefly explained in the appendix. In section 3 we present our results and discuss them in section 4.

2. Model and numerical method

In the present work the NMF model is defined by the following equations of state written in terms of the mean site magnetizations $\{m_i\}$ and the corresponding free energy F_{NMF} without specifying any underlying explicit spin model:

$$m_i = \tanh\beta\Bigg(\sum_j J_{ij}m_j + h_i\Bigg) \tag{1}$$

$$F_{\mathrm{NMF}} = \frac{1}{2\beta}\sum_i\left\{(1+m_i)\ln\left(\frac{1+m_i}{2}\right) + (1-m_i)\ln\left(\frac{1-m_i}{2}\right)\right\} - \sum_{(ij)} J_{ij}m_im_j - \sum_i h_im_i \tag{2}$$

where $\beta = 1/T$, h_i is the external magnetic field on site i, and the infinite-ranged interactions $\{J_{ij}\}$ are Gaussian random variables with mean zero and variance $J^2/(N-1)$, N being the total number of spins in the system.

Our numerical procedures are as follows. First, all metastable states at $T = 0$ in each sample are prepared by checking stabilities of all spin configurations against one spin-flip process [5]. This step is most time consuming and restricts the size of systems we can examine. Then, using each metastable state thus found as an initial configuration, we look for a stationary solution of the following equations of relaxational dynamics at finite temperatures

$$-\tau\frac{\mathrm{d}m_i}{\mathrm{d}t} = m_i - \tanh\beta\Big(\sum_j J_{ij}m_j + h_i\Big). \tag{3}$$

The temperatures are increased stepwise. The value of τ is chosen such that the iterative method to solve equation (3) works most effectively. The convergence to a stationary solution is judged by the criterion $N^{-1}\sum_i(\Delta m_i^a)^2 < 10^{-6}$, where Δm_i^a is the change of m_i^a by one iteration step. The two solutions $\{m_i^a\}$ and $\{m_i^b\}$ thus obtained are regarded as identical if the conditions $|q_a - q_b| < 10^{-3}$ and $1 - |\tilde{q}_{ab}| < 10^{-3}$ are satisfied†, where $q_a = q_{aa}$, $\tilde{q}_{ab} = q_{ab}/(q_a q_b)^{1/2}$, and q_{ab} is the overlap parameter defined by $q_{ab} \equiv N^{-1}\sum_i m_i^a m_i^b$. If any branch of a metastable state which appears once at a finite temperature persists down to $T = 0$ as a solution for equations (1), including the case that it bifurcates into several branches, the present numerical method starting from all the solutions at $T = 0$ is also expected to exhaust all the metastable states at finite temperatures. The results obtained and described in later sections support, though they cannot prove, this expectation.

Typical numbers of samples examined are 2000, 1000, 500, and 200 for N =12, 16, 20, and 24, respectively. The energy and temperature are scaled by J so that the transition temperature $T_c = 2$ in the thermodynamic limit. The step of the temperature increase is set to 0.05. In this work we examine the equations of state under the vanishing magnetic field $h_i = 0$ only.

3. Results

Let us start with analyses of the numbers of metastable states, N_S, at finite T. The system-size dependences of $\log\langle N_S\rangle_J$ are plotted for some T in figure 1(a), where $\langle\ldots\rangle_J$ indicates the average over samples. The data are fitted to the following empirical form

$$\ln\langle N_S\rangle_J = \phi N + A + BN^{-n}. \tag{4}$$

with $n = 1/3$. The resulting ϕ are presented in figure 1(*b*). The number of metastable states, and so ϕ in the thermodynamic limit ($N \to \infty$) can be evaluated by the method of Bray and Moore [3] as briefly explained in the appendix. The result is also drawn by the solid curve in the figure. The agreement between the two results is surprisingly

† The second criterion for $\tilde{q}_{ab}$ implies that we pick up, as for a solution of equations (1), only one of the two solutions which are symmetric with each other against the time reversal transformation. Although the overlaps q_{ab} between the two solutions thus selected are not necessarily non-negative, we simply put $q_{ab} = |q_{ab}|$ in evaluating the Parisi order parameter $\bar{q}$ and the overlap probability $P_J(q)$ (equations (5*b*) and (8) later).

well in spite of the fact that $\langle N_S \rangle_J$ are rather small (for example, as seen in figure 1(a), $\langle N_S \rangle_J \simeq 4.5$ at $T = 0.5$ even for systems with $N = 24$). In this context it is noted that at lowest temperatures, where $\langle N_S \rangle_J$ are rather large, the fitting even to a straight line (without the last term in equation (4)) gives rise to the ϕ value within the error bars in figure 1(b). We regard this agreement as a support that our numerical method almost exhausts all the metastable states at finite temperatures.

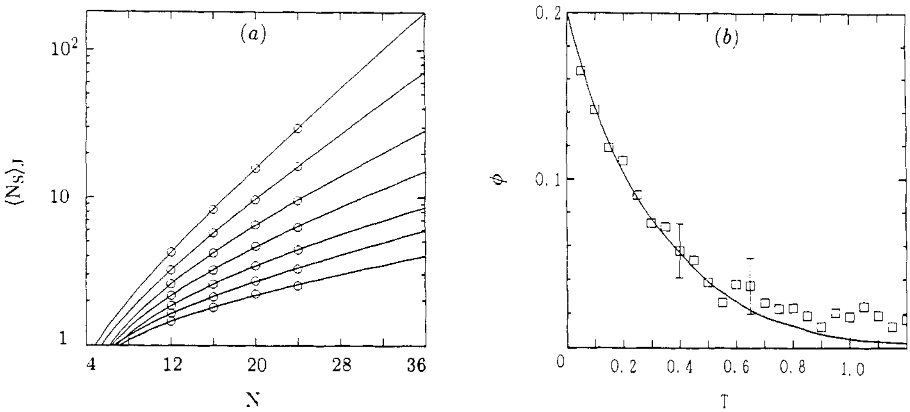

Figure 1. Numbers of metastable states $\langle N_S \rangle_J$. (a) Their dependence on system size, N, at several temperatures in intervals of 0.1 (from $T = 0.1$ (top) to $T = 0.7$ (bottom)). The curves are the fits to equation (4) with $n = 1/3$. (b) Temperature dependence of ϕ in equation (4) obtained from the fits. The full curve indicates the analytical result in the thermodynamic limit [5].

It is worth noting how metastable states disappear as the temperature is increased. Most of the processes are the confluence of a metastable state to another with a large drop of free-energy. We may interpret it as disappearance of a valley which was located within a larger valley and had a rather high free energy relative to the bottom at the preceding temperature. The process is hard to regard as the inverse of bifurcation of a metastable state in cooling process. We expect that 'bifurcation scenario' of metastable states proposed by Mézard *et al* [12] can be applied to metastable states with lowest free energies and is hardly ascertained by the present numerical analysis on small systems.

Making use of the solutions selected as described in section 2, we have evaluated the Edwards–Anderson (EA) order parameter q_{EA} and the Parisi order parameter $\bar{q}$ defined respectively by

$$q_{\mathrm{EA}} = \left\langle \sum_a P_a q_a \right\rangle_J \tag{5a}$$

$$\bar{q} = \left\langle \sum_{ab} P_a P_b q_{ab} \right\rangle_J \tag{5b}$$

where the weight P_a is given by

$$P_a \equiv \frac{\exp(-\beta F^a_{\mathrm{NMF}})}{Z} \tag{6}$$

and $Z \equiv \sum_a \exp(-\beta F^a_{\rm NMF})$. For each T we have examined the variance of $q_{\rm EA}$ and confirmed that it is self-averaging, i.e., the variance decreases in proportion to N^{-a}, where a is nearly equal to 1 within the present numerical accuracy. Its averages $q_{\rm EA}(N)$ are then fitted to an empirical form $q_{\rm EA}(N) = q^\infty_{\rm EA} + C/N$. From the data for $\bar{q}(N)$, on the other hand, its asymptotic limit $\bar{q}^\infty$ is hardly estimated. The results of $q^\infty_{\rm EA}$, $\bar{q}(12)$ and $\bar{q}(24)$ are shown in figure 2. At lowest temperatures $q_{\rm EA}$ and $\bar{q}$ for each N exhibit the following asymptotic forms:

$$q_{\rm EA} \simeq 1 - aT^{3/2} \tag{7a}$$

$$\bar{q} \simeq 1 - T + \bar{a}T^{3/2} \tag{7b}$$

with $a \simeq \bar{a}$.

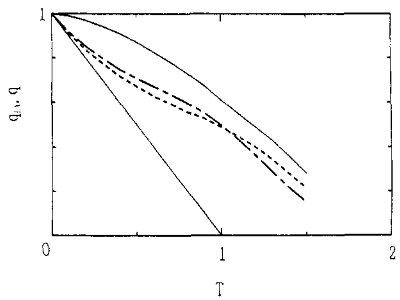

Figure 2. Temperature dependence of the order parameters $q_{\rm EA}$ and $\bar{q}$. The full, chain and broken curves represent $q^\infty_{\rm EA}$, $\bar{q}$ for $N = 24$ and $\bar{q}$ for $N = 12$ respectively. The full line indicates $\bar{q}^{\rm SK}$ $(= 1 - T)$.

Next we examine the overlap probability $P_J(q)$ defined by

$$P_J(q) = \sum_{ab} P_a P_b \delta(q - q_{ab}) \tag{8}$$

and the accumulated probabilities $x_J(q)$ and $Y_J(q)$. Typical results of its average $P(q)$ $(\equiv \langle P_J(q)\rangle_J)$ are shown in figure 3(a). As N increases the peak in $P(q)$ at around $q = q_{\rm EA}$ sharpens, but the tail part below $q_{\rm EA}$ remains finite. The former is the sum of the self-overlap of each metastable state, while the latter is attributed to the overlaps between different metastable states. In figure 3(b) we plot the inverse of the corresponding function $x(q)$ $(\equiv \langle x_J(q)\rangle_J)$, namely, the order parameter function $q(x)$. For comparison, we draw also $q(x)$ of the SK model with $q(1) = q_{\rm EA} \simeq 0.82$ (at $T = 0.25$). At lowest temperatures both $q(x)$'s can be approximated as

$$q(x) \simeq \begin{cases} x/2\alpha & x \lesssim x_T = 2\alpha \\ q_{\rm EA} & x_T \lesssim x \leq 1 \end{cases} \tag{9}$$

where α is a constant. Then $\bar{q}$ is approximately evaluated as $\bar{q} \simeq q_{\rm EA} - \alpha$. For the SK model Parisi's solution yields exactly $\bar{q}^{\rm SK} = 1 - T$. Therefore $\alpha_{\rm SK}$ should be given by $\alpha_{\rm SK} \simeq T - (1 - q^{\rm SK}_{\rm EA})$. $q^{\rm SK}_{\rm EA}$ is known to behave $q^{\rm SK}_{\rm EA} \simeq 1 - cT^2$, c being a constant. For the NMF model, on the other hand, equation (7) with $a \simeq \bar{a}$ implies

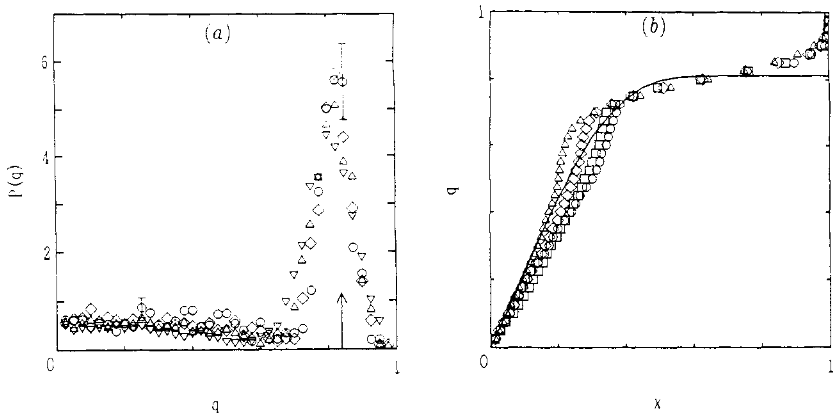

Figure 3. (a) The overlap probability $P(q)$ at $T = 0.6$ for various system sizes: $N = 24$ (○), 20 (◇), 16 (△) and 12 (▽). The arrow represents the value of q_{EA}^{∞} at this temperature. (b) The corresponding function $q(x)$, i.e., the inverse of accumulated probability $x(q)$. The full curve represents $q(x)$ of the SK model with $q(1) \simeq 0.82$ (at $T = 0.25$) evaluated from Parisi's replica-symmetry-broken solution.

$\alpha_{\mathrm{NMF}} \simeq T - 2(1 - q_{\mathrm{EA}}^{\mathrm{NMF}})$. $q_{\mathrm{EA}}^{\mathrm{NMF}}$ is given by $q_{\mathrm{EA}}^{\mathrm{NMF}} \simeq 1 - c(T/2)^{3/2}$, where $c \simeq 1.0$ from our numerical analysis in the limit $N \to \infty$, while $c \simeq 1.4$ from the replica analysis described in the appendix. These differences in the α seen in figure 3(b) as well as in the q_{EA} can be attributed to the Onsager term which is present only in the TAP equations.

Lastly we examine the probability law of the accumulated probability $Y_J(q)$. For the SK model it is predicted by the replica method [12] that $Y_J(q)$ is not self-averaging and that its distribution law is universal in the sense that the moments $\langle Y_J^n(q)\rangle_J$ are expressed as a function of the first moment y ($\equiv \langle Y_J(q)\rangle_J$) alone:

$$Y_2 \equiv \langle Y_J^2(q)\rangle_J = \tfrac{1}{3}(y + 2y^2) \tag{10a}$$

$$Y_3 \equiv \langle Y_J^3(q)\rangle_J = \tfrac{1}{15}(3y + 7y^2 + 5y^3) \tag{10b}$$

and so on. In the phase space representation $Y_J(q)$ is rewritten as

$$Y_J(q) = \sum_{ab} P_a P_b \theta(q_{ab} - q) \tag{11}$$

where $\theta(x)$ is the step function. For the SK model $Y_J(q_{\mathrm{EA}})$ is known to reduce

$$Y_J(q_{\mathrm{EA}}) = \sum_a P_a^2 \equiv W_J. \tag{12}$$

The right-hand side of the expression is interpreted as the inverse 'participation ratio' of the weights $\{P_a\}$. These ratios W_J obey also the above probability law for the SK model.

Having all the metastable states in hand, we can directly calculate the above moments $\langle Y_J^n(q)\rangle_J$ as well as $\langle W_J^n\rangle_J$ of the NMF model at finite temperatures. The results for the second and third moments are shown in figures 4(a) and 4(b), respectively. It is noted that if there is only one metastable state (excluding its time-reversal state)

$Y_J(q) = \theta(q_{EA} - q)$ and so we obtain $Y_2 = Y_3 = y$. Such data are in fact obtained at higher temperatures, but they are excluded from the figures. The data points presented in the figures clearly do not lie on the self-averaging curves given by $Y_2 = y^2$ and $Y_3 = y^3$. More interestingly, they are almost on the curves given by equations (10*a*) and (10*b*), namely, the probability law of $Y_J(q)$ (and W_J) of the NMF model coincides with that of the SK model. This result is the first numerical evidence for the universal probability law of $Y_J(q)$, and at the same time it expands the concept of the universality to the system whose equations of states are different from the SK model.

The data in figure 4 are concentrated to the range $y > 0.5$. This is in agreement with the replica argument [12] that the most probable value of $Y_J(q)$ is unity, and means that among the weights $\{P_a\}$ only a few of them are dominant. Does this also mean that the rest of the metastable states whose number is huge as shown in figure 1 are entirely irrelevant to the spin glass properties? In order to answer this question we have examined the organization of metastable states from a different point of view. Besides the complete scan of the phase space, we have also carried out the $T = 0$ Monte Carlo analysis to find out the solutions at $T = 0$. By this method the lower energy states are reached to the more frequently. This indicates that each lower energy state is associated with a relatively large size of basin of attractor if the spin dynamics is governed by the $T = 0$ Monte Carlo process (rapid cooling). To measure size of the basins we analyse the probability $p_a \equiv M_a/M$, where M_a is the number of trials which end up with the ath state and M the number of total random trials. In the insets of figure 4 the moments of its inverse 'participation ratio' $Y_A \equiv \sum_a p_a^2$ are also plotted. The data have small $\langle Y_A \rangle_J$ and are rather close to the self-averaging curves. Also $\langle Y_A \rangle_J$ tends to vanish in the limit $N \to \infty$.

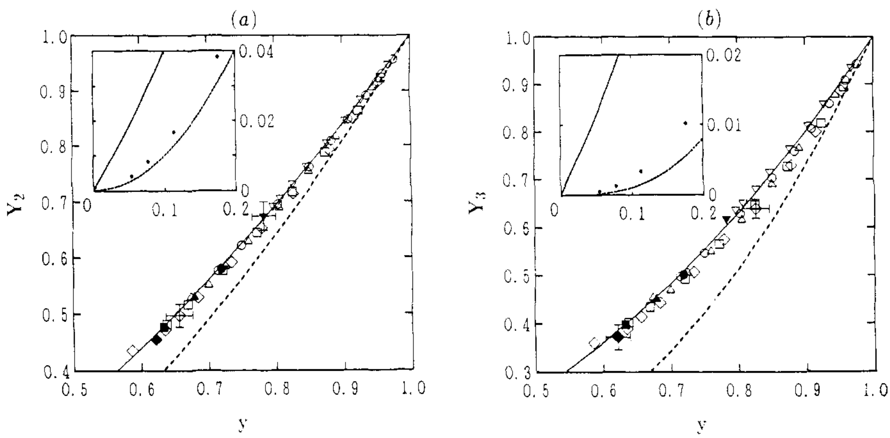

Figure 4. (*a*) The second and (*b*) third moments of $Y_J(q)$ and W_J of systems with $N = 24$. The open (full) symbols are for $Y_J(q)$ (W_J). Each symbol represents the data obtained at the same temperature; $T = 0.2$ (○, ●), 0.4 (□, ■), 0.6 (◇, ◆), 0.8 (△, ▲), and 1.0 (▽, ▼). The full and broken curves represent equations (10) and the self-averaging curves, respectively. Insets the corresponding moments of Y_A of systems with $N = 12$ (top), 16, 20 and 24 (bottom) are shown by the data points.

4. Discussions

Combining all the observations described in the preceding sections we may conclude with the following picture for the statistical-mechanical organization of metastable states in the NMF model. There are a large number (which is however much smaller than N_S in figure 1) of metastable states having lower energies. They have almost equivalent weights if the system is cooled rapidly. Since, however, differences in the (free) energies, each of which is of the order of N, are much larger than the temperature of interest, only a few lowest (free) energy states dominates in quantities averaged by the weights $\{P_a\}$. It is then expected that gradual cooling (or simulated annealing) selects one of a few lowest free-energy states which are 'reproducible', i.e. their thermodynamic quantities are independent of the states. It is also these lowest free energy states with significant weights $\{P_a\}$ that give rise to the universal probability law of $Y_J(q)$. A large number of metastable states with lower energies are considered to play a fundamental role on the hysteretic phenomena which exhibit much more variety and subtlety than those in ordinary ferromagnets.

The spin glass properties obtained here for the NMF model are initially predicted for the SK model [1]. The two models are described by different equations of state and so have different thermodynamic behaviours such as the spin-glass order parameters $\bar{q}$ and q_{EA} discussed below equation (9). We emphasize further the following difference. Metastable states in the SK model locate just on the edge of the validity condition of the TAP equations [6], while those in the NMF model locate far from the region where the Hessian matrix of the free energy becomes negative (see figure 1 in [8]). The common spin glass properties obtained in the two models in spite of these differences are thus considered intrinsic ones at least to mean-field spin glasses, and might be so to spin glasses with short-ranged interactions [10].

Lastly a comment is in order on the implication of the present results with the properties of spin glasses with short-ranged interactions. The present work strongly support that the method of Bray and Moore [3, 8] counts appropriately the averaged number of metastable states $\langle N_S\rangle_J$ in mean-field models for spin glasses. According to the method, ϕ in $\langle N_S\rangle_J = \exp(N\phi)$ is given by

$$\phi \cong \gamma\epsilon^6 \tag{13}$$

near T_c, where $\epsilon = 1 - (T/T_c)$, and $\gamma = 8/81$ for the SK model [3] and $\gamma = 128/21$ for the NMF model [8]. Then at $T = 0.8T_c$ $N\phi$ of the SK model becomes 0.02 even with $N = 14^3$ so that we may hardly obtain non-trivial overlap probability $P(q)$ in such a finite system. To the contrary, Caracciolo *et al* [10] have observed non-trivial $P(q)$ at $T = 0.83T_c$ in 3D Ising spin glasses even with $N = 6^3, 10^3$ and 14^3. This means that there are relatively more metastable states in 3D Ising spin glasses than in mean-field models at temperatures close to T_c, which contradicts our simpleminded expectation. Although we cannot judge their criterion of equilibration in detail from their article, one possible interpretation is that metastable states claimed by Caracciolo *et al* might not strictly be 'pure states' but they are still organized, if observed by an appropriate time scale, as those in the mean-field spin glasses. There exists, however, no satisfactory theory yet to answer this problem.

Acknowledgments

We thank Dr F R Waugh for his correspondence about his group's work related to [11]. The numerical work was done at Scientific Information Processing Center, University of Tsukuba. This work was financially supported by a Grant-in-Aid for Scientific Research from the Ministry of Education, Science and Culture, Japan.

Appendix

By the replica trick developed by Bray and Moore [3], the averaged number of metastable states $\langle N_S \rangle_J$ in the NMF model is given by (we put $l = \frac{1}{2}$, $\gamma = 0$ and $B/2 \to B$ in the corresponding equations in [8])

$$\langle N_S \rangle_J = \mathrm{Max}_{[\lambda,q,B,\Delta,\sigma]}\{\exp(N\phi)\} \tag{A.1}$$

$$\phi = -\lambda q + \tfrac{1}{2}t^2(4B^2 - \Delta^2 - 4\sigma B - 2\sigma^2) + \ln\mathcal{J} \tag{A.2}$$

$$\mathcal{J} = \int_{-\infty}^{\infty} \frac{\mathrm{d}z}{(2\pi)^{\frac{1}{2}}} \frac{\{1 + B(1-m^2)\}^{3/2}}{\{1 + (B+\sigma)(1-m^2)\}^{1/2}} \exp\left[-\frac{1}{2}\left(z - \frac{t\Delta}{q^{1/2}} m \right)^2 + \lambda m^2 \right] \tag{A.3}$$

where $t = T/T_{\mathrm{c}}$ and $m = \tanh(\beta J q^{1/2} z)$. The saddle-point conditions for the parameters $\lambda, q, B, \sigma, \Delta$ are given by equations (2.8) in [8].

At temperatures higher than a certain critical temperature $t_{\mathrm{c}}(\cong 0.225)$ the above equations can be solved straightforwardly by numerical iteration. At t_{c} B reaches -1 and the saddle-point stability starts to be broken in a certain range of z. Therefore, in our previous analysis [8], we fixed B at $-1 + \epsilon$ (ϵ being an infinitesimal positive constant) and solved for the other parameters and evaluated ϕ below t_{c}. A better method for getting out of the saddle-point instability is proposed by Waugh *et al* [11], namely in the integration in equation (A.3) the range of z where the saddle point is unstable $(1 + B(1 - m^2) < 0)$ is to be discarded. Then the asymptotic behaviour of the parameters in the limit $t \to 0$ are given by $q \simeq 1 - 2\eta^{1/2}t^{3/2}$, $\lambda \simeq -\eta^2/2 \simeq -\sigma$, $\Delta \simeq \eta t^{-1}$, $B \simeq -\eta^{1/2}t^{-1/2}$, where $\eta \cong 0.506$. Then ϕ is evaluated as $\phi \simeq -(t\Delta)^2/2 + \ln\mathcal{J} \cong 0.199$. As compared with our previous results [8], the asymptotic behaviour of B, σ and $1 - q$ are different, but those of Δ and λ, and therefore ϕ are identical. In particular, the ϕ of the two analyses coincide with each other over the whole range below t_{c} within our numerical accuracy.

References

[1] Mézard M, Parisi G and Virasoro M A 1987 *Spin Glass Theory and Beyond* (Singapore: World Scientific)
[2] Bray A J and Moore M A 1979 *J. Phys. C: Solid State Phys.* **12** L441
[3] Bray A J and Moore M A 1980 *J. Phys. C: Solid State Phys.* **13** L469
[4] Parga N, Parisi G and Virasoro M A 1984 *J. Physique Lett.* **45** L1063
[5] Nemoto K 1988 *J. Phys. A: Math. Gen.* **21** L287
[6] Nemoto K and Takayama H 1985 *J. Phys. C: Solid State Phys.* **18** L529
[7] Bray A J, Sompolinsky H and Yu C 1986 *J. Phys. C: Solid State Phys.* **19** 6389
[8] Takayama H and Nemoto K 1990 *J. Phys.: Condens. Matter* **2** 1997
[9] Sourlas N 1988 *Europhys. Lett.* **6** 561
[10] Caracciolo S, Parisi G, Patarnello S and Sourlas N 1990 *Europhys. Lett.* **11** 783
[11] Waugh F R, Marcus C M and Westervelt R M 1990 *Phys. Rev. Lett.* **64** 1986
[12] Mézard M, Parisi G, Sourlas N, Toulouse G and Virasoro M 1984 *J. Physique* **45** 843
[13] Young A P 1983 *Phys. Rev. Lett.* **51** 1206
[14] Nemoto K 1987 *J. Phys. C: Solid State Phys.* **20** 1325